# Screening of Protein-Ligand Binding using a SABRE Hyperpolarized Reporter

Ratnamala Mandal,[‡] Pierce Pham,[‡] Christian Hilty*

Department of Chemistry, Texas A&M University, 3255 TAMU, College Station, TX 77843, USA

‡ these authors contributed equally

*corresponding author: chilty@tamu.edu

## Abstract

Hyperpolarization through Signal Amplification by Reversible Exchange (SABRE) provides a facile means to enhance NMR signals of small molecules containing an N-heterocycle or other binding site for a polarization transfer catalyst. A purpose-designed reporter ligand, which is capable of binding both to a target protein and to the catalyst, makes the sensitivity enhancement by this technique compatible with the measurement of a range of biomolecular interactions. The $^{1}$H polarization of the reporter ligand 4-amidinopyridine, which is targeting trypsin, is used to screen ligands that are not themselves hyperpolarizable by SABRE. The respective protein-ligand dissociation constants ($K_D$) are determined by an observed change in the $R_2$ relaxation rate of the reporter. A calculation of expected signal changes indicates that the accessible ligand $K_D$ values extend over several orders of magnitude, while the concentrations of target proteins and ligands can be reduced considering the sensitivity gains from hyperpolarization. In general, the design of a single, weakly binding ligand for a target protein enables the use of SABRE hyperpolarization for ligand screening or other biophysical studies involving macromolecular interactions.

## Introduction

Nuclear magnetic resonance (NMR) offers significant benefits for the characterization of the binding of ligands to proteins with applications in screening for drug discovery. Specifically, NMR observable parameters such as $R_2$ relaxation,[1,2] nuclear Overhauser effect,[3,4] chemical shift,[5,6] and others, are sensitive to the binding interaction. Subsets of these parameters can be used to identify binding, characterize binding affinities or determine binding site structures. Nuclear spin hyperpolarization

techniques overcome a low sensitivity of acquired signals, which is otherwise the most significant drawback of the use of NMR for ligand binding studies. A high signal enhancement, on the order of hundreds or thousands-fold allows for a reduction in the ligand and, concomitantly also of the protein concentration to what would be physiologically relevant levels. The signal enhancement also provides a contrast for the selective observation of the compound of interest over the non-hyperpolarized background. Hyperpolarization by dissolution dynamic nuclear polarization (D-DNP)[7] has previously been proposed for improving the ability to detect ligand binding, measuring binding affinity and dynamics, and determining bound structures.[8–13]

Recently, we demonstrated the application of another hyperpolarization method, the *para*-hydrogen[14] based signal amplification by reversible exchange (SABRE),[15] providing a facile alternative for producing ligand hyperpolarization.[16] SABRE requires that the molecule to be hyperpolarized bind to a polarization transfer catalyst directly, or that it receives hyperpolarization through exchange of protons *via* another ligand in the SABRE-Relay process.[17,18] SABRE proceeds through a mechanism that depends on the *J*-couplings and frequency differences, which are described by the level anti-crossing theory.[19] These requirements can be satisfied by selecting the magnetic field used for polarization, for $^{1}$H polarization in the milli-Tesla range. Additionally, the SABRE process depends on favorable exchange rates between the catalyst bound and free forms of the substrate.[20] The exchange rates for substrates with different steric size and electron densities at the binding site can be optimized by the choice of the other ligands in the Ir complex.[21–24]

We recently demonstrated the application of SABRE for characterizing protein-ligand interactions with a molecule, 4-amidinopyridine, which contains binding sites for both the polarization transfer catalyst and the trypsin protein.[16] In a two-step mechanism, the hyperpolarization was produced under separately optimizable conditions, using a typical SABRE catalyst [Ir(IMeMes)(COD)]Cl[21] (IMeMes=1-(2,4,6-trimethylphenyl)-3-methylimidazol-2-ylidene, COD=cyclooctadiene) in methanol solution. A small aliquot of the hyperpolarized liquid was then mixed with the protein solution, diluting the organic solvent to a final concentration of several percent and allowing NMR spectroscopy with the protein in its native form.

Here, we show that NMR of SABRE hyperpolarized small molecules has a broader applicability to determine biomolecular interactions between a wide variety of biological molecules that are not necessarily hyperpolarizable through SABRE. Through competitive binding, the signals from a fast-

exchanging ligand can report on another molecular interaction, as the fast exchanging ligand becomes displaced.[25] Thus, only a single small molecule needs to be hyperpolarized as a reporter ligand.[8] It is anticipated that for most proteins, a weakly binding ligand can be found or modified to contain a binding site for a SABRE polarization transfer catalyst, thus enabling the use of this hyperpolarization method for screening libraries of ligands, or for other biophysical investigations of the target protein.

## Experimental Section

*Para*-hydrogen was produced by passing room temperature hydrogen over iron (III) oxide spin-flip catalyst (Sigma-Aldrich, St. Louis, MO) in a heat exchanger immersed in liquid nitrogen at the temperature of 77 K. The para content was 50% as determined from the ratios of the signal intensities of ortho-hydrogen in the *para*-hydrogen enriched and from room-temperature equilibrated hydrogen.[26]

The sample for hyperpolarization consisted of 0.3 mM of the asymmetric precatalyst [Ir(IMeMes)(COD)]Cl and 1.5 mM ligand 4-amidinopyridine hydrochloride (Alfa Aesar, Ward Hill, MA) in methanol-$d_4$ (Cambridge Isotope Libraries, Andover, MA). The precatalyst was synthesized according to a previously established protocol.[21] For the activation of the precatalyst, *para*-hydrogen (~50% *para*-content) was bubbled through the sample at a pressure of $8.3 \cdot 10^5$ Pa and at 294 K. The SABRE hyperpolarization was conducted in a 6.5 mT magnetic field that was generated by a solenoid coil (diameter 22 cm and length 28 cm). The non-hyperpolarized sample consisted of 50 mM sodium phosphate buffer in $D_2O$ (pH=7.6) and 1 mM 2,2'-bipyridine, or of buffer, 2,2'-bipyridine and 40 µM trypsin. For the competition experiments, the competing ligands of interest (500 µM benzylamine, 500 µM benzamidine or 30 µM leupeptin) were included. 5 mM sodium trimethylsilylpropanesulfonate (DSS) was included as a reference compound in the non-hyperpolarized sample.

After the hyperpolarization was established, the sample was delivered to a sample loop using the pressure of the hydrogen gas. Subsequently, the sample was taken to a flow-cell that was pre-installed in the 9.4 T magnet using a high-pressure syringe pump (Model 500D Teledyne Isco, Lincoln, NE). The injector device used for this purpose is described elsewhere.[27] At the same time, the non-hyperpolarized sample was injected using another high pressure syringe pump (Model 1000D, Teledyne Isco). The two samples mixed in a Y-mixer before entering the magnet with a mixing time $t_{mix}$ of 1.05 s. For the NMR experiments, a single scan Carr-Purcell-Meiboom-Gill (CPMG) experiment was performed to determine the $R_2$ relaxation rates of the $^1$H spins of the 4-amidinopyridine ligand. Before acquiring the echoes, water suppression was achieved by applying EBURP pulses of 20 ms

duration to excite the water signals, and dephasing them by pulsed field gradients. A pulsing delay of 1696.2 µs was used in the CPMG block, and 64 points were collected per echo. The total experiment time was 10.4 s.

The echoes measured from the CPMG experiments were multiplied with time symmetric dual exponential window functions and Fourier transformed. The spectra were phased with a constant phase correction value maximizing the real part of the spectrum. A reference water signal (sample without ligand) was subtracted from each echo by scaling to the maximum solvent signal intensity. The ligand signal was then integrated (peak ~8.1 ppm) and fitted to a single exponential curve to obtain the $R_2$ rates from each experiment.

The concentrations in the competitive binding experiment were determined after the CPMG experiment from the same samples in the flow cell. The concentration of the reporter ligand $[R]_0$ was determined by referencing the $^1$H NMR signal intensities to a sample of 20 mM of the ligand 4-amidinopyridine in the same flow cell. For the determination of the concentration of the competing ligand $[C]_0$ and protein $[P]_0$, the reference DSS signal was used. The dilution factor was determined based on the $^1$H NMR signal intensity of DSS and was used to determine the final concentrations, $[C]_0$ and $[P]_0$.

The dissociation constant of the reporter ligand $K_{D,r}$ and the total concentrations of reporting ligand $[R]_0$ and protein $[P]_0$ were used to determine bound fraction of reporter ligand in non-competition experiment $p_{b,r}^{(nc)}$ (SI equations 1.5 and 1.6b). The bound fraction of reporting ligand in competition experiment $p_{b,r}^{(c)}$ was calculated from the relative fraction of the bound reporter ligand $f$ and the $p_{b,r}^{(nc)}$ value (SI equation 1.7).

The $p_{b,r}^{(c)}$, $[R]_0$ and $[P]_0$ values were used to calculate the apparent dissociation constant of the reporter ligand, and using the competing ligand total concentration $[C]_0$, to calculate the dissociation constant of the competing ligand $K_{D,c}$ (SI equations 1.9 and 1.10).

## Results and Discussion

The molecule 4-amidinopyridine (Figure 1a) serves as the reporter ligand for the protein trypsin in the later competing experiments. This molecule was injected into an NMR flow cell (Figure 1b) after hyperpolarization with the asymmetric SABRE catalyst [Ir(IMeMes)(COD)]Cl,[21] as previously described[16,27] (see Experimental Section). The proton spin relaxation rates of 4-amidinopyridine in the presence and absence of protein were determined from single-scan Carr-Purcell-Meiboom-Gill (CPMG) experiments. The chelating ligand 2,2'-bipyridine[28] was mixed with the hyperpolarized

sample during injection, before the data acquisition. Trapping the catalyst with the chelating ligand alleviates relaxation contributions due to interactions with the reporter ligand, which would be detrimental to the identification of protein binding.[16]

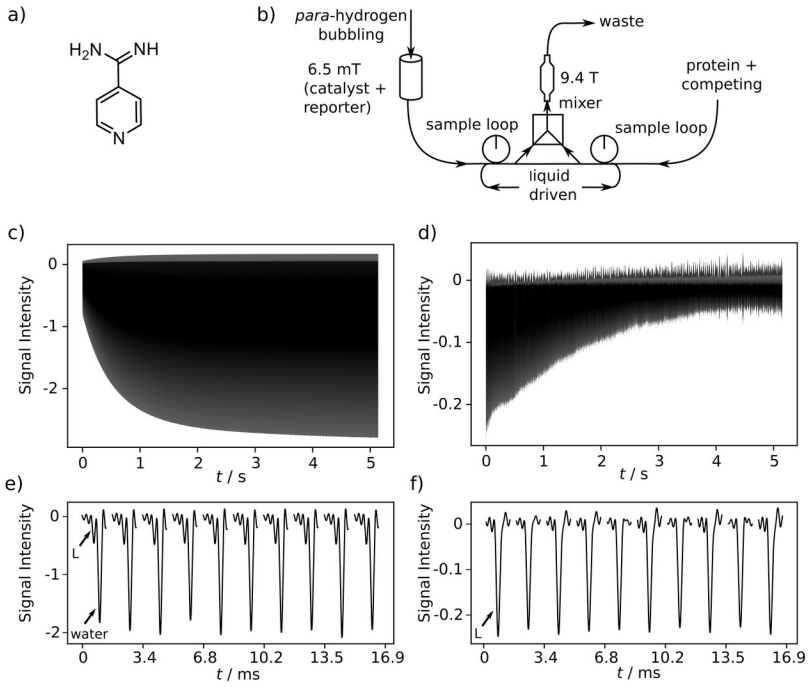


***Figure 1.*** *a) Structure of the reporter ligand 4-amidinopyridine. b) Schematic representation of the flow-NMR setup for ligand-binding characterization using SABRE. c) Series of spectra corresponding to 3000 CPMG echoes (τ = 1.7 ms) for the reporter ligand (144 μM 4-amidinopyridine) without water subtraction. d) Series of spectra from (c) after water subtraction. e and f) First 10 spectra from (c) and (d) shown enlarged. The chemical shifts of reporter ligand (L) and water are indicated.*

Figure S1a in SI shows the real part of a CPMG echo that is multiplied with an exponential window function (Figure S1b in SI) before being Fourier transformed into an NMR spectrum. The water peak at ~4.7 ppm is the largest in this spectrum; therefore, a separately measured reference water signal (Figure S1f) is subtracted from the hyperpolarized ligand signal. The largest peak in the spectrum after water subtraction (Figure S1g), at a chemical shift of 8.1 ppm, contains the signals from both aromatic protons of the 4-amidinopyridine. These signals are not individually resolved due to the short echo time

of 1.7 ms, which results in a spectral resolution of 590 Hz. A signal enhancement of ~100-fold for the reporter ligand facilitates its observation in the presence of the non-hyperpolarized water. A series of spectra corresponding to 3000 CPMG echoes (0 - 5.1 s) is plotted in Figure 1c, and the first 10 spectra are shown in Figure 1e. Because the water chemical shift is off resonance during implementing CPMG pulse train, the imperfect π pulses on the water signal cause the partially excitation of its $I_z$ component. This effect leads to the growth of water signal with respect to time in Figure 1c, rather than the decay due to $R_2$ relaxation. This artifact is removed by applying water subtraction from these spectra, and the results are shown in Figures 1d and 1f. As expected for a SABRE experiment, the signal of the reporter ligand has an initially negative intensity and subsequently relaxes towards the negligibly small positive intensity at thermal equilibrium.

The relaxation process is visible in the signal intensities shown in Figure 2a, which are integrated from a single CPMG echo train. In some of the spectra, a second peak from the suppressed water signal is visible near 4.7 ppm. A faster relaxation is observed in the presence of protein, due to averaging of the relaxation rate of the free ligand fraction with the faster rate of the bound fraction (Figures 2b and 2d). Fitting of a single exponential to the relaxation data resulted in a transverse relaxation rate of 144 μM free reporter ligand, $R_{2,r}^{(f)} = 0.47 \pm 0.01\ s^{-1}$. In the presence of 11.7 μM trypsin, the relaxation rate for the non-competing reporter ligand increased to $R_{2,r}^{(nc)} = 1.86 \pm 0.13\ s^{-1}$.

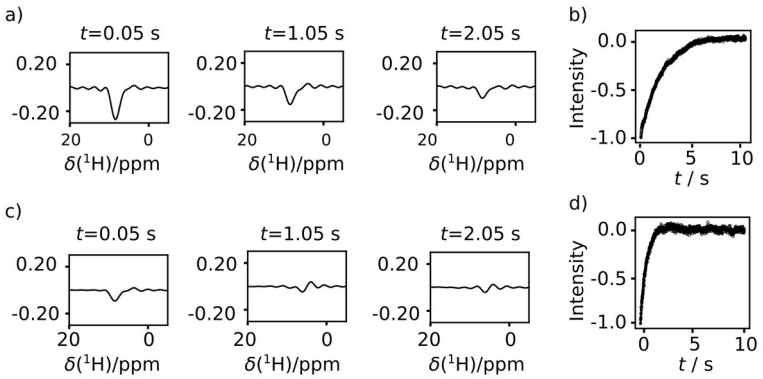


***Figure 2.*** *a) Spectra of hyperpolarized reporter ligand 4-amidinopyridine after Fourier transformation of echoes and water subtraction, in the absence of trypsin. b) Echo signal intensities from (a) with fit indicating a relaxation rate of 0.48 $s^{-1}$ (data set shown) for the free ligand. R2 values from three separate measurements were 0.47 ± 0.01 $s^{-1}$. c) Spectra of hyperpolarized 130 μM 4-amidinopyridine in the presence of 11.7 μM trypsin, obtained from CPMG echoes as in (a). d) Fit of the data in (c),*

*indicating a relaxation rate of 1.89 $s^{-1}$ (data set shown; 1.86 ± 0.13 $s^{-1}$ from three measurements) in the presence of trypsin.*

Relaxation rates of the same molecule 4-amidinopyridine were measured when a second ligand for the protein, the competing ligand of interest, was included with the protein solution. Figure 3 shows the signal integrals resulting from screening the ligands of interest benzylamine, benzamidine and leupeptin. The corresponding spectra from CPMG echo trains, when 4-aminidopyridine is in competition, are shown in Figures S3 - S5 in SI. As these ligands partially displace the reporter ligand, its observed relaxation rate changes. The relaxation rate of the reporter ligand after displacement falls in-between the rates for free reporter and reporter with protein alone.[8,25] The weakest ligand of interest, benzylamine, was present at a concentration of 166 μM to achieve partial displacement manifested as an observable change in the relaxation rate (Figure 3a). In contrast, the strongly binding leupeptin caused a large change in $R_2$ relaxation at the much lower concentration of 7 μM (Figure 3c). The partial displacement of the reporter ligand, barring allosteric effects, indicates that the ligand of interest binds to the same binding site of the protein as the reporter ligand.

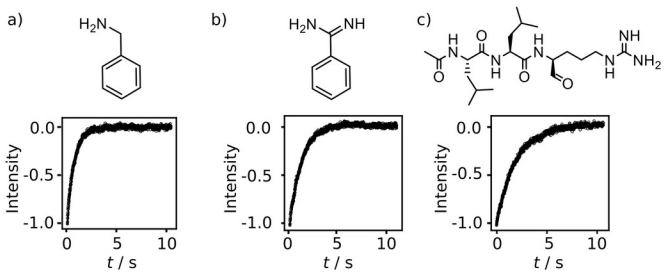


***Figure 3.*** *Structures of competing ligands and $R_2$ relaxation rates from CPMG experiments for the reporter ligand 4-amidinopyridine measured in the presence of competing ligands (a) 161 μM 4-amidinopyridine with 166 μM benzylamine, 14.7 μM trypsin and chelating agent 2,2'-bipyridine (b) 146 μM 4-amidinopyridine with 136 μM benzamidine, 13 μM trypsin and chelating agent 2,2'-bipyridine and (c) 140 μM 4-amidinopyridine with 7 μM leupeptin, 8.4 μM trypsin and chelating agent 2,2'-bipyridine. The fitted relaxation rates in competition, $R_{2,r}^{(c)}$, are 1.52 $s^{-1}$, 0.85 $s^{-1}$ and 0.55 $s^{-1}$ for the data sets shown in (a), (b) and (c) respectively (1.47 ± 0.04 $s^{-1}$, 0.88 ± 0.06 $s^{-1}$ and 0.58 ± 0.05 $s^{-1}$, respectively, from three measurements).*

Under the solution conditions of the experiments, the relaxation rate in competition, $R_{2,r}^{(c)}$, determined from three separate measurements was fastest with benzylamine at 1.47 ± 0.04 $s^{-1}$, followed by benzamidine at 0.88 ± 0.06 $s^{-1}$, and leupeptin at 0.58 ± 0.05 $s^{-1}$ (Table S1 in SI). These rates indicate that in the first experiment, the smallest fraction of reporter ligand was displaced, with increasing fractions in the second and third experiment.

The level of displacement depends on the concentrations and on the dissociation constants of both the reporter and competing ligands. If the dissociation constant of the reporter ligand, $K_{D,r}$, is known, it can be used to determine the dissociation constant of the competing ligand of interest, $K_{D,c}$. The $K_{D,r}$ was independently determined to be 152 ± 51 μM from NMR titrations (Figure S6 in SI). The $K_{D,c}$ values of the competing ligands were then determined following ref. [8], resulting in 200 ± 80 μM for benzylamine, 28 ± 8 μM for benzamidine and 0.27 ± 0.14 μM for leupeptin. These $K_{D,c}$ values and associated error ranges were estimated based on the averages and standard deviations of the $R_2$ values from the three separate measurements, as well as the separately measured $K_{D,r}$ value. The determined values for $K_{D,c}$ correspond to previously reported values of 258.1 ± 56.6 μM, 16.3 ± 1.6 μM and 0.09 ± 0.03 μM for the three ligands, respectively.[8] The slightly weaker affinity measured here for the latter two ligands may be due to the presence of the <10% methanol in the final solution.

An additional error in the measured $K_{D,c}$ can be introduced by binding of the reporter ligand to the polarization transfer catalyst. Although the catalyst is trapped by 2,2'-bipyridine during the NMR measurement, a remaining open coordination site may bind a ligand molecule, potentially causing changes in concentration or relaxation. There was no significant difference in $R_2$ values between non-hyperpolarized experiments without catalyst,[16] and SABRE experiments with inactivated catalyst. It can be inferred that the exchange rates of the free and catalyst-bound reporter ligands were too slow to contribute to the observed relaxation. However, the catalyst may sequester ligand at a 1:1 ratio.[28] Accounting for the resulting reduction in free ligand concentration would cause the $K_{D,c}$ values to increase by at most 10%. This contribution to the measured values is neglected in the above discussion.

For a successful determination of $K_{D,c}$ from the experiment, the ligand and protein concentrations should be chosen to cause a partial displacement of the reporter ligand and, consequently, a relaxation rate that is different from the rates of free reporter and reporter in presence of the protein alone. The optimal concentration ranges can be predicted from calculating the relative fraction of bound reporter ligand in the competing and non-competing experiments, $f = p_{b,r}^{(c)}/p_{b,r}^{(nc)}$ (SI equations 1.2 – 1.7). In

Figure 4a, the fraction *f* is shown for given concentrations of the protein and reporter ligand similar to the experimental conditions. The concentration of the competing ligand is varied along the vertical, and the dissociation constant of the competing ligand, $K_{D,c,}$ along the horizontal axis. Conditions with *f* values in the range of 0.2 – 0.8, reflective of the desired partial displacement,[29] are enclosed by the dash-dotted curves. The concentrations of the three competing ligands used in the experiments are indicated in the figure according to their determined $K_{D,c}$ values, falling within this range.

Under conditions where the fraction of bound reporter ligand is small and the reporter ligand is in fast exchange, *f* equals the value $\alpha = (R_{2,r}^{(c)} - R_{2,r}^{(f)}) / (R_{2,r}^{(nc)} - R_{2,r}^{(f)})$. The parameter $\alpha$ is calculated solely from the experimentally determined transverse relaxation rates. Based on Monte Carlo simulations and error analysis, it was previously concluded that the most reliable value of $K_{D,c}$ can be obtained when the $\alpha$ value is near 0.5.[8]

The concentration limits for optimal determination of $K_{D,c}$ in general depend on the relative values of the dissociation constants of the reporter and competing ligands. This dependence is illustrated in Figure 4b, which shows the *f* values in cross-sections along the horizontal axis of Figure 4a. For strongly binding ligands such as leupeptin, the optimal *f* values are achieved at a lower concentration and in a narrower concentration range compared to the weaker ligands.

Under the present experimental conditions, irrespective of $K_{D,c}$ values, a competing ligand concentration of ~1 μM or lower does not cause a significant displacement of the bound reporter ligand and should not be used for $K_{D,c}$ determination. Figure S7 explores, for this protein and ligand system, how lowering the concentrations of protein or reporter ligand may allow a concomitant reduction of the competing ligand concentration. Decreasing reporter concentration (top to bottom in Figure S7) does not significantly alter the *f* values but increases the fraction of bound reporter. On the other hand, the optimal *f* values for strongly binding competitors can be achieved at the concentrations of ~1 μM and ~0.1 μM by lowering protein concentrations 10– and 100– fold, respectively (left to right in Figure S7), but the fraction of bound reporter is also significantly reduced. This reduction lessens the observed change of $R_2$ relaxation. Therefore, it is critical to consider all concentrations to not only obtain an appropriate *f* value but also a significant fraction of bound reporter.

When 4-amidinopyridine was hyperpolarized at a concentration of 1.5 mM, signal enhancement values close to 100–fold could be achieved using 50% *para*-enriched $H_2$. After dilution and mixing with the non-hyperpolarized sample, a final sample concentration of ~150 μM was achieved for the reporter

ligand. As discussed in ref. [16], increasing the *para*-percentage to 99% and further modifications in the experimental setup would enable lowering the final concentration of 4-amidinopyridine to 20 µM or less, and the protein concentration to the sub-micromolar range. This in turn would allow to further lower the concentration of the competing ligand in accordance with the above discussion.

Compared to benzamidine, a widely reported ligand for trypsin, the chosen reporter ligand contains an additional N-atom in the aromatic ring. This change in structure is required, as benzamidine cannot be hyperpolarized by SABRE. At the same time, the change in the structure facilitates the use of the molecule as a reporter ligand by reducing its affinity for the protein. A ligand of low affinity is in fast exchange with the protein, which is a requirement for the competitive binding experiment. In general, although drug candidates or other molecules of biological interest may not themselves be SABRE hyperpolarizable, the described method requires only a single weakly binding reporter ligand for characterizing the binding of any other ligand to the same site of the protein. The reporter ligand may be found by modifying a known ligand for the target protein as for 4-amidinopyridine vs. benzamidine employed here. Additionally, computational methods may be utilized to identify a weakly binding ligand *in silico*.[30] Relevant methods include combining docking with molecular dynamics simulations and determination of free energies for the protein-ligand interaction.[31]

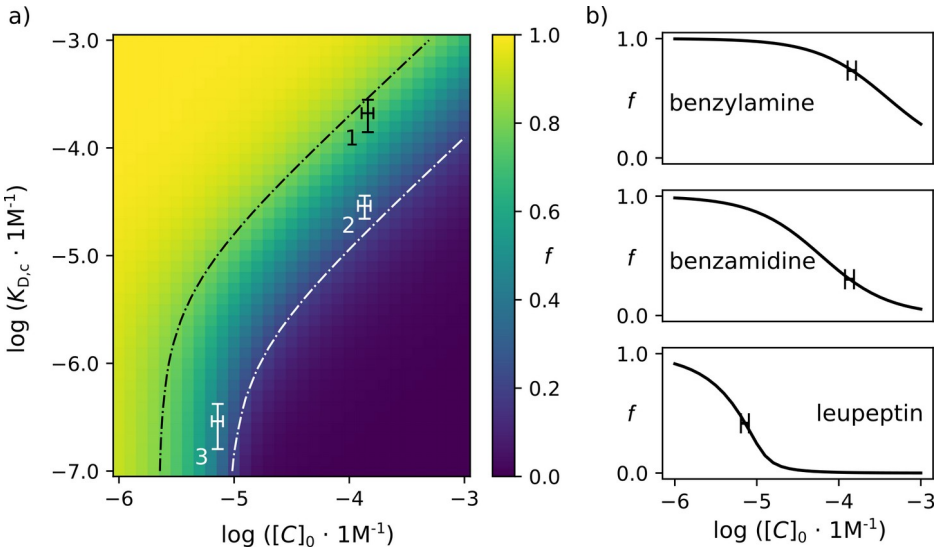


***Figure 4.*** *a) The calculated relative fraction of the bound reporter between the competition and non-competition experiments, $f = p^{b,r}{}_{(c)}/p^{b,r}{}_{(nc)}$, plotted as a function of competitor concentration $[C]_0$ and dissociation constant $K_{D,c}$ of the competing ligand of interest. For the calculation, a total concentration*

*$[P]_0$ = 11 µM of tryspin, $[R]_0$ = 145 µM of the reporter ligand, and $K_{D,r}$ = 152 µM were used. The experimental conditions are indicated for benzylamine ("1", $[C]_0$ = 145 ± 17 µM, $K_{D,c}$ = 200 ± 70 µM), benzamidine ("2", $[C]_0$ = 136 ± 17 µM, $K_{D,c}$ = 28 ± 7 µM), and leupeptin ("3", $[C]_0$ = 7.2 ± 0.8 µM, $K_{D,c}$ = 0.27 ± 0.13 µM). The f values in the range of 0.2 – 0.8 are enclosed by dash-dotted curves. b) Horizontal cross-sections extracted from (a) at the $K_{D,c}$ values for the three ligands.*

With the measurement of $R_2$ relaxation under competitive binding, the dissociation constant of a ligand of interest can be determined. Thus, a single reporter ligand will allow the screening of a library of potential ligands to determine whether they bind to the protein, and to measure the binding affinity. This task is a common application of NMR in drug discovery. The ability to continuously produce SABRE hyperpolarization for a reporter ligand mixture, in combination with additional improvements of the injection device such as autosampling and possible complementary strategies including parallelized detection[32] or immobilization of target proteins[33,34] would enable true high-throughput screening using this method. The time required per sample may be reduced to close to the NMR scan time on the order of tens of seconds or less.

SABRE polarization enhances the signals of $^{1}$H in the molecule to be detected by several orders of magnitude. In the experiments described here, the increased signal facilitated distinguishing these signals from the water peak even in spectra acquired from echoes with short echo time, and after additional water suppression at a water proton concentration that was up to $10^5$ times larger than the signals to be detected. In other applications, the signal enhancement from this hyperpolarization method could also be used to identify the molecule to be detected in the presence of other, abundant signals. It can become possible to measure biomolecular interactions in samples containing many different components, even without requiring purification. In such applications, the hyperpolarization can be used in a similar way as an isotope label would be applied with an isotope filtered conventional NMR experiment.[35,36] However, the use of $^{1}$H SABRE hyperpolarization does not require the synthesis of compounds incorporating $^{13}$C or $^{15}$N labels, which is often difficult or expensive. In addition to $^{1}$H, SABRE can also be used to hyperpolarize other nuclei. The aforementioned $^{15}$N or $^{13}$C nuclei in molecules such as pyridine or pyruvate have been polarized using the SABRE-SHEATH method, which employs a magnetic shield to reduce the ambient field to the µT range during the polarization step.[37,38] Additionally, $^{19}$F in heterocyclic rings can be hyperpolarized by the same method. $^{19}$F has an

intrinsically high natural isotope abundance, and therefore does not require enrichment. Significant $^{19}$F signal enhancements of molecules such as 3-fluoropyridine, >100-fold, have been described.[39] Fluorine atoms are abundant in drug molecules and drug lead compounds. Approximately 20% of commercial pharmaceuticals contain this nucleus, with many possessing fluorine-substituted nitrogen heterocyclic compounds.[40] The abundance of such structural motifs indicates the potential of using $^{19}$F SABRE hyperpolarization for investigating protein-ligand interactions. With $^{19}$F detection, NMR spectra are background-free, and thus do not require solvent subtraction techniques such as described in Figure 1, which would further simplify the experiment.

Apart from detecting the interaction of small molecules with a protein, the method based on a small-molecule reporter ligand hyperpolarized by SABRE is applicable to other biophysical studies. These include the characterization of enzymes, as well as the determination of macromolecular interactions, such as protein-protein or protein-nucleic acid interactions that cause the displacement of a ligand.

## Conclusion

In summary, we demonstrated the screening of protein-ligand interactions, benefitting from substantial sensitivity enhancements provided by SABRE hyperpolarization. Only a single hyperpolarizable reporter ligand that binds weakly to the protein is required to measure the binding affinity of a wide range of ligands of interest. This capability significantly expands the applicability of SABRE for biomolecular applications. The combination of the protein and SABRE hyperpolarizable reporter can serve as a basis for high-throughput screening of protein-ligand interactions. Additionally, this method is amenable to other biophysical studies involving molecular or macromolecular interactions of the target protein.

## Supporting Information

The Supporting Information is available free of charge at https://pubs.acs.org/

Experimental; Measured Data Sets; Experimental Parameters and Values; Dissociation Constant ($K_{D,r}$) of Reporter Ligand; Calculated Binding Parameters; References

## Conflicts of Interest

Texas A&M University is filing a patent application covering parts of this work.

## Acknowledgments

Financial support from the National Science Foundation (Grant CHE-1900406) and the Welch Foundation (Grant A-1658) is gratefully acknowledged.

## References

(1) Hajduk, P. J.; Olejniczak, E. T.; Fesik, S. W. One-Dimensional Relaxation- and Diffusion-Edited NMR Methods for Screening Compounds That Bind to Macromolecules. *J. Am. Chem. Soc.* **1997**, *119* (50), 12257–12261. https://doi.org/10.1021/ja9715962.

(2) Nitsche, C.; Otting, G. NMR Studies of Ligand Binding. *Curr. Opin. Struct. Biol.* **2018**, *48*, 16–22. https://doi.org/10.1016/j.sbi.2017.09.001.

(3) Chen, W.-N.; Nitsche, C.; Pilla, K. B.; Graham, B.; Huber, T.; Klein, C. D.; Otting, G. Sensitive NMR Approach for Determining the Binding Mode of Tightly Binding Ligand Molecules to Protein Targets. *J. Am. Chem. Soc.* **2016**, *138* (13), 4539–4546. https://doi.org/10.1021/jacs.6b00416.

(4) Constantine, K. L.; Davis, M. E.; Metzler, W. J.; Mueller, L.; Claus, B. L. Protein−ligand NOE Matching: A High-Throughput Method for Binding Pose Evaluation That Does Not Require Protein NMR Resonance Assignments. *J. Am. Chem. Soc.* **2006**, *128* (22), 7252–7263. https://doi.org/10.1021/ja060356w.

(5) Arai, M.; Ferreon, J. C.; Wright, P. E. Quantitative Analysis of Multisite Protein–Ligand Interactions by NMR: Binding of Intrinsically Disordered P53 Transactivation Subdomains with the TAZ2 Domain of CBP. *J. Am. Chem. Soc.* **2012**, *134* (8), 3792–3803. https://doi.org/10.1021/ja209936u.

(6) Williamson, M. P. Using Chemical Shift Perturbation to Characterise Ligand Binding. *Prog. Nucl. Magn. Reson. Spectrosc.* **2013**, *73*, 1–16. https://doi.org/10.1016/j.pnmrs.2013.02.001.

(7) Ardenkjaer-Larsen, J. H.; Fridlund, B.; Gram, A.; Hansson, G.; Hansson, L.; Lerche, M. H.; Servin, R.; Thaning, M.; Golman, K. Increase in Signal-to-Noise Ratio of > 10,000 Times in Liquid-State NMR. *Proc. Natl. Acad. Sci.* **2003**, *100* (18), 10158–10163. https://doi.org/10.1073/pnas.1733835100.

(8) Kim, Y.; Hilty, C. Affinity Screening Using Competitive Binding with Fluorine-19 Hyperpolarized Ligands. *Angew. Chem. Int. Ed.* **2015**, *54* (16), 4941–4944. https://doi.org/10.1002/anie.201411424.

(9) Lee, Y.; Zeng, H.; Ruedisser, S.; Gossert, A. D.; Hilty, C. Nuclear Magnetic Resonance of Hyperpolarized Fluorine for Characterization of Protein–Ligand Interactions. *J. Am. Chem. Soc.* **2012**, *134* (42), 17448–17451. https://doi.org/10.1021/ja308437h.

(10) Lerche, M. H.; Meier, S.; Jensen, P. R.; Baumann, H.; Petersen, B. O.; Karlsson, M.; Duus, J. Ø.; Ardenkjær-Larsen, J. H. Study of Molecular Interactions with 13C DNP-NMR. *J. Magn. Reson.* **2010**, *203* (1), 52–56. https://doi.org/10.1016/j.jmr.2009.11.020.

(11) Qi, C.; Wang, Y.; Hilty, C. Application of Relaxation Dispersion of Hyperpolarized 13C Spins to Protein–Ligand Binding. *Angew. Chem. Int. Ed.* **2021**, *60* (45), 24018–24021. https://doi.org/10.1002/anie.202109430.

(12) Cioffi, M.; Hunter, C. A.; Packer, M. J.; Spitaleri, A. Determination of Protein–Ligand Binding Modes Using Complexation-Induced Changes in $^{1}$H NMR Chemical Shift. *J. Med. Chem.* **2008**, *51* (8), 2512–2517. https://doi.org/10.1021/jm701194r.

(13) Buratto, R.; Mammoli, D.; Chiarparin, E.; Williams, G.; Bodenhausen, G. Exploring Weak Ligand-Protein Interactions by Long-Lived NMR States: Improved Contrast in Fragment-Based Drug Screening. *Angew. Chem. Int. Ed.* **2014**, *53* (42), 11376–11380. https://doi.org/10.1002/anie.201404921.
(14) Bowers, C. R.; Weitekamp, D. P. Transformation of Symmetrization Order to Nuclear-Spin Magnetization by Chemical Reaction and Nuclear Magnetic Resonance. *Phys. Rev. Lett.* **1986**, *57* (21), 2645–2648. https://doi.org/10.1103/PhysRevLett.57.2645.
(15) Adams, R. W.; Aguilar, J. A.; Atkinson, K. D.; Cowley, M. J.; Elliott, P. I. P.; Duckett, S. B.; Green, G. G. R.; Khazal, I. G.; Lopez-Serrano, J.; Williamson, D. C. Reversible Interactions with Para-Hydrogen Enhance NMR Sensitivity by Polarization Transfer. *Science* **2009**, *323* (5922), 1708–1711. https://doi.org/10.1126/science.1168877.
(16) Mandal, R.; Pham, P.; Hilty, C. Characterization of Protein–Ligand Interactions by SABRE. *Chem. Sci.* **2021**, *12* (39), 12950–12958. https://doi.org/10.1039/D1SC03404A.
(17) Roy, S. S.; Appleby, K. M.; Fear, E. J.; Duckett, S. B. SABRE-Relay: A Versatile Route to Hyperpolarization. *J. Phys. Chem. Lett.* **2018**, *9* (5), 1112–1117. https://doi.org/10.1021/acs.jpclett.7b03026.
(18) Iali, W.; Rayner, P. J.; Duckett, S. B. Using Parahydrogen to Hyperpolarize Amines, Amides, Carboxylic Acids, Alcohols, Phosphates, and Carbonates. *Sci. Adv.* **2018**, *4* (1), eaao6250. https://doi.org/10.1126/sciadv.aao6250.
(19) Ivanov, K. L.; Pravdivtsev, A. N.; Yurkovskaya, A. V.; Vieth, H.-M.; Kaptein, R. The Role of Level Anti-Crossings in Nuclear Spin Hyperpolarization. *Prog. Nucl. Magn. Reson. Spectrosc.* **2014**, *81*, 1–36. https://doi.org/10.1016/j.pnmrs.2014.06.001.
(20) Cowley, M. J.; Adams, R. W.; Atkinson, K. D.; Cockett, M. C. R.; Duckett, S. B.; Green, G. G. R.; Lohman, J. A. B.; Kerssebaum, R.; Kilgour, D.; Mewis, R. E. Iridium N-Heterocyclic Carbene Complexes as Efficient Catalysts for Magnetization Transfer from Para-Hydrogen. *J. Am. Chem. Soc.* **2011**, *133* (16), 6134–6137. https://doi.org/10.1021/ja200299u.
(21) Wong, C. M.; Fekete, M.; Nelson-Forde, R.; Gatus, M. R. D.; Rayner, P. J.; Whitwood, A. C.; Duckett, S. B.; Messerle, B. A. Harnessing Asymmetric N-Heterocyclic Carbene Ligands to Optimise SABRE Hyperpolarisation. *Catal. Sci. Technol.* **2018**, *8* (19), 4925–4933. https://doi.org/10.1039/c8cy01214h.
(22) Colell, J. F. P.; Logan, A. W. J.; Zhou, Z.; Lindale, J. R.; Laasner, R.; Shchepin, R. V.; Chekmenev, E. Y.; Blum, V.; Warren, W. S.; Malcolmson, S. J.; Theis, T. Rational Ligand Choice Extends the SABRE Substrate Scope. *Chem. Commun.* **2020**, *56* (65), 9336–9339. https://doi.org/10.1039/D0CC01330G.
(23) Pham, P.; Hilty, C. Tunable Iridium Catalyst Designs with Bidentate N-Heterocyclic Carbene Ligands for SABRE Hyperpolarization of Sterically Hindered Substrates. *Chem. Commun.* **2020**, *56* (98), 15466–15469. https://doi.org/10.1039/D0CC06840C.
(24) Stanbury, E. V.; Richardson, P. M.; Duckett, S. B. Understanding Substrate Substituent Effects to Improve Catalytic Efficiency in the SABRE Hyperpolarisation Process. *Catal. Sci. Technol.* **2019**, *9* (15), 3914–3922. https://doi.org/10.1039/C9CY00396G.
(25) Dalvit, C.; Flocco, M.; Knapp, S.; Mostardini, M.; Perego, R.; Stockman, B. J.; Veronesi, M.; Varasi, M. High-Throughput NMR-Based Screening with Competition Binding Experiments. *J. Am. Chem. Soc.* **2002**, *124* (26), 7702–7709. https://doi.org/10.1021/ja020174b.
(26) Hövener, J.-B.; Pravdivtsev, A. N.; Kidd, B.; Bowers, C. R.; Glöggler, S.; Kovtunov, K. V.; Plaumann, M.; Katz-Brull, R.; Buckenmaier, K.; Jerschow, A.; Reineri, F.; Theis, T.; Shchepin, R. V.; Wagner, S.; Bhattacharya, P.; Zacharias, N. M.; Chekmenev, E. Y. Parahydrogen-Based

Hyperpolarization for Biomedicine. *Angew. Chem. Int. Ed.* **2018**, *57* (35), 11140–11162. https://doi.org/10.1002/anie.201711842.
(27) Chen, H.-Y.; Hilty, C. Implementation and Characterization of Flow Injection in Dissolution Dynamic Nuclear Polarization NMR Spectroscopy. *ChemPhysChem* **2015**, *16* (12), 2646–2652. https://doi.org/10.1002/cphc.201500292.
(28) Mewis, R. E.; Fekete, M.; Green, G. G. R.; Whitwood, A. C.; Duckett, S. B. Deactivation of Signal Amplification by Reversible Exchange Catalysis, Progress towards in Vivo Application. *Chem. Commun.* **2015**, *51* (48), 9857–9859. https://doi.org/10.1039/C5CC01896J.
(29) Fielding, L. NMR Methods for the Determination of Protein–Ligand Dissociation Constants. *Prog. Nucl. Magn. Reson. Spectrosc.* **2007**, *51* (4), 219–242. https://doi.org/10.1016/j.pnmrs.2007.04.001.
(30) Tinberg, C. E.; Khare, S. D.; Dou, J.; Doyle, L.; Nelson, J. W.; Schena, A.; Jankowski, W.; Kalodimos, C. G.; Johnsson, K.; Stoddard, B. L.; Baker, D. Computational Design of Ligand-Binding Proteins with High Affinity and Selectivity. *Nature* **2013**, *501* (7466), 212–216. https://doi.org/10.1038/nature12443.
(31) Wang, J.; Guo, Z.; Fu, Y.; Wu, Z.; Huang, C.; Zheng, C.; Shar, P. A.; Wang, Z.; Xiao, W.; Wang, Y. Weak-Binding Molecules Are Not Drugs?—Toward a Systematic Strategy for Finding Effective Weak-Binding Drugs. *Brief. Bioinform.* **2017**, *18* (2), 321–332. https://doi.org/10.1093/bib/bbw018.
(32) Kim, Y.; Liu, M.; Hilty, C. Parallelized Ligand Screening Using Dissolution Dynamic Nuclear Polarization. *Anal. Chem.* **2016**, *88* (22), 11178–11183. https://doi.org/10.1021/acs.analchem.6b03382.
(33) Wang, Y.; Hilty, C. Amplification of Nuclear Overhauser Effect Signals by Hyperpolarization for Screening of Ligand Binding to Immobilized Target Proteins. *Anal. Chem.* **2020**, *92* (20), 13718–13723. https://doi.org/10.1021/acs.analchem.0c01071.
(34) Vanwetswinkel, S.; Heetebrij, R. J.; van Duynhoven, J.; Hollander, J. G.; Filippov, D. V.; Hajduk, P. J.; Siegal, G. TINS, Target Immobilized NMR Screening: An Efficient and Sensitive Method for Ligand Discovery. *Chem. Biol.* **2005**, *12* (2), 207–216. https://doi.org/10.1016/j.chembiol.2004.12.004.
(35) Wang, Y.; Ragavan, M.; Hilty, C. Site Specific Polarization Transfer from a Hyperpolarized Ligand of Dihydrofolate Reductase. *J. Biomol. NMR* **2016**, *65* (1), 41–48. https://doi.org/10.1007/s10858-016-0037-x.
(36) Wang, Y.; Hilty, C. Determination of Ligand Binding Epitope Structures Using Polarization Transfer from Hyperpolarized Ligands. *J. Med. Chem.* **2019**, *62* (5), 2419–2427. https://doi.org/10.1021/acs.jmedchem.8b01711.
(37) Theis, T.; Truong, M. L.; Coffey, A. M.; Shchepin, R. V.; Waddell, K. W.; Shi, F.; Goodson, B. M.; Warren, W. S.; Chekmenev, E. Y. Microtesla SABRE Enables 10% Nitrogen-15 Nuclear Spin Polarization. *J. Am. Chem. Soc.* **2015**, *137* (4), 1404–1407. https://doi.org/10.1021/ja512242d.
(38) TomHon, P.; Abdulmojeed, M.; Adelabu, I.; Nantogma, S.; Kabir, M. S. H.; Lehmkuhl, S.; Chekmenev, E. Y.; Theis, T. Temperature Cycling Enables Efficient $^{13}$C SABRE-SHEATH Hyperpolarization and Imaging of [1-$^{13}$C]-Pyruvate. *J. Am. Chem. Soc.* **2022**, *144* (1), 282–287. https://doi.org/10.1021/jacs.1c09581.
(39) Chukanov, N. V.; Salnikov, O. G.; Shchepin, R. V.; Svyatova, A.; Kovtunov, K. V.; Koptyug, I. V.; Chekmenev, E. Y. $^{19}$F Hyperpolarization of $^{15}$N-3-$^{19}$F-Pyridine via Signal Amplification by Reversible Exchange. *J. Phys. Chem. C* **2018**, *122* (40), 23002–23010. https://doi.org/10.1021/acs.jpcc.8b06654.

(40) Inoue, M.; Sumii, Y.; Shibata, N. Contribution of Organofluorine Compounds to Pharmaceuticals. *ACS Omega* **2020**, *5* (19), 10633–10640. https://doi.org/10.1021/acsomega.0c00830.